Solar Energy Materials & Solar Cells 95 (2011) 1638–1646

Contents lists available at ScienceDirect

Solar Energy Materials & Solar Cells

journal homepage: www.elsevier.com/locate/solmat

Modeling of the nominal operating cell temperature based on outdoor weathering

Michael Koehl*, Markus Heck, Stefan Wiesmeier, Jochen Wirth

Fraunhofer ISE, Heidenhofstr. 2, 79110 Freiburg, Germany

ARTICLE INFO

Article history:
Received 27 April 2010
Received in revised form
11 January 2011
Accepted 13 January 2011
Available online 25 February 2011

Keywords:
Module temperature
Nominal operating cell temperature
Outdoor exposure
Modeling of temperature
PV-module

ABSTRACT

Simple analytical and statistical models for the evaluation of the temperature of PV-modules from climatic data (ambient temperature, global solar irradiation, and wind speed) are investigated. The parameters which describe the effects of cell technology and module design were evaluated from outdoor exposure data at different climatic regions. The models were validated by comparison of the simulated module temperatures with measured module temperatures at different test sites. A simplified way to determine a Realistic Nominal Module Temperature (ROMT) instead of the Nominal Operating Cell Temperature (NOCT) is proposed.

1. Introduction

The efficiency of photovoltaic cells depends on the cell temperature, which is usually described by temperature coefficients for the current, the voltage, and the power. These temperature coefficients are different for different cell technologies. The energy rating of PV systems can make use of meteorological data for the investigated location, but needs additional information about the cell temperature or the module temperature. This temperature itself is influenced by the optical properties of the modules' components (cells, glazing, encapsulant, back-sheets), the electrical efficiency of the cells and the heat-transfer to the ambient, depending of the ambient climatic conditions like ambient temperature, wind, irradiation, and the properties relevant for radiative heat transfer like albedo, sky temperature and orientation of the module. Moreover, the temperature conditions of the module are strongly influenced by the thermal insulation of the module back-side resulting from the roof-mounting or building integration. We do not consider the mounting situation here, but focus on freestanding modules.

The so-called Nominal Operating Cell Temperature (NOCT), which is defined by IEC standards [2] as the cell temperature in a module exposed at 45° south to 800 W/m^2 irradiation at 20 °C ambient temperature and with wind at a speed of about 1 m/s, should characterize the temperature dependence. However, the exposure conditions are "open circuit", which do not account for the electrical energy withdrawal that leads to disadvantages for modules with high efficiency. Further, it is not efficient to use NOCT for energy rating with transient climatic conditions. A model for the description of the correlation between solar irradiation, ambient temperature, and wind, and the module temperature would be more useful. What is more, the evaluation of the NOCT according to the standards requires tough border conditions for the ambient climate, which could not often be met at the testing laboratories for some months during bad weather seasons. The resulting delays during module type approval testing are not appreciated by the customers.

The temperature is also very important for the degradation of the PV-modules, because it determines at least the reaction rate for the degradation processes caused by the other degradation factors (hydrolysis by humidity and photo-degradation by UV-light, e.g.). Modeling of the service life of modules applied in different climatic regions requires time series of the module temperature.

A model which allows calculating the module temperature as function of the ambient temperature, the global irradiation, and the wind speed, would facilitate the use of any time series of climatic data for a climatic region of interest, which could be provided by weather services, test reference years or via the internet.

2. Outdoor monitoring

Different test sites (see Fig. 1) have been equipped with instrumentation for monitoring the climate. The solar irradiance

* Corresponding author.
E-mail address: michael.koehl@ise.fraunhofer.de (M. Koehl).

0927-0248/$ - see front matter © 2011 Elsevier B.V. All rights reserved.
doi:10.1016/j.solmat.2011.01.020

Nomenclature

a	coefficient describing the effect of the radiation on the module temperature in the King-model
b	coefficient describing the cooling by the wind in the King-model (s/m)
G	global irradiation in the plane of incidence (W/m^2)
H	normalized irradiation (°C)
T_{mod}	module temperature (°C)
T_{amb}	ambient temperature (°C)
U_0	W/°C m^2 coefficient describing the effect of the radiation on the module temperature in the Faiman model
U_1	Ws/°C m^3 coefficient describing the cooling by the wind in the Faiman model
v	wind speed (m/s)

Subscripts

mod	module
amb	ambient

Units

h	hours
K	Kelvin
kWh/m^2	energy per meter square
m	meter
min	minutes
m/s	velocity
s	second
W	Watt
W/m^2	power density of the incident solar irradiation
°C	degrees Celsius
°	degrees
%	percent

Abbreviations

AM	air-mass
a-Si	amorphous silicon
BIPV	building-integrated photovoltaics
CdTe	cadmium telluride
CIS	copper indium gallium selenide
FWHM	full width at half maximum
IEC	International Electrotechnical Commission
NOCT	Nominal Operating Cell Temperature
PCR	Principle Component Regression
ROMT	Realistic Operating Module Temperature

was measured by calibrated pyranometers, UV-A, UV-B with integral sensors; the wind velocity, and direction with anemometers 3 m above ground, except for the NOCT measurements in Freiburg, where the wind was measured according to IEC61215 close to the modules in the plane of the modules by means of an ultra-sonic anemometer. The module temperatures were measured at the back-sheets by means of foil Pt-100 sensors except at the site in Sede Boqer, where thermo-couples were used. The measurement results were stored as 5-min averages [1].

Seven module-types based on crystalline solar cells were exposed. Resistive loads keep them in operation near the so-called maximum power point. The electrical power is dumped in the resistor in this case, reducing the temperature load for the modules.

Different thin-film modules were investigated within the scope of the EU-project PERFORMANCE in subproject 5 (Service life assessment). Triplicates of each kind were exposed for outdoor weathering with monitoring of the module temperatures and the climatic data at the CEA/INES research station in Cadarache (France) and at Fraunhofer ISE in Freiburg (Germany), as shown in Fig. 1 upper left. All modules were equipped with electronic loads for alternating IU-monitoring and mpp-tracking.

3. Data evaluation

The frequency distributions of the average module temperatures at three different test sites show the wide variety of the climatic conditions (Fig. 2). The average module temperature was 65 °C at the maximum, about 30 K above ambient temperature (Fig. 3), and shows the radiation cooling resulting in module temperatures up to 6 K below ambient, clearly to be seen in Fig. 4.

The difference between module temperature and ambient temperature is nearly a linear function of the irradiation with a slope depending on the wind speed (see Fig. 5). Deviations can be observed for low and high irradiations. Radiation cooling and natural convection reduces the module temperature for a small wind speed (lower than about 4 m/s) and low solar irradiation. The higher the wind speed, the smaller the deviation caused by these cooling effects. Natural convection reduces the temperature at very high irradiation and low wind speed. Turbulent heat transfer above 7 m/s wind speed might be assumed when the module temperature not really depends on the wind speed.

4. Modeling of module temperatures

The energy rating of PV systems can make use of meteorological data for the investigated location, but needs additional information about the module temperature. The temperature dependence of the module efficiency primarily depends on the type of cells. The cell temperature itself is influenced by the optical properties of the other components (glazing, encapsulant, back-sheets) and the ambient climatic conditions. The so-called Nominal Operating Cell Temperature (NOCT), which is defined by IEC standards [2] as the cell temperature in a module exposed at 45° south to 800 W/m^2 irradiation at 20 °C ambient temperature and with wind at a speed of about 1 m/s, should characterize the temperature dependence. However, it is not efficient to use NOCT for energy rating with transient climatic conditions. A model for the description of the correlation between solar irradiation, ambient temperature and wind and the module temperature would be more useful.

Numerous models were proposed for the simulation of the module temperature. A comprehensive overview is given in [3].

Here, we focus on two models. One model was presented by David King [4]. Without taking into account the temperature difference between back-side and cell from the original expression

$$T_{mod} = T_{amb} + H\exp(-a-bv) \quad (1)$$

where H is a normalized irradiation with the dimension of °C, like the ambient and the module temperature, and a is a dimensionless coefficient describing the effect of the radiation on the module temperature, while b describes the cooling by the wind and has the dimension s/m.

Fig. 1. The outdoor test facilities: City (upper left): Freiburg, Germany (equipped with thin-film modules and reference modules), Desert (upper right): Sede Boqer, Israel, in cooperation with the Ben-Gurion University of the Negev and TÜV Rheinland; Alps: Schneeferner Haus, Germany (middle left), in cooperation with TÜV Rheinland; Tropics (middle right): Serpong, Indonesia, in cooperation with TÜV Rheinland; Maritime (lowest picture): Gran Canaria, in cooperation with Instituto Technologico de Canarias.

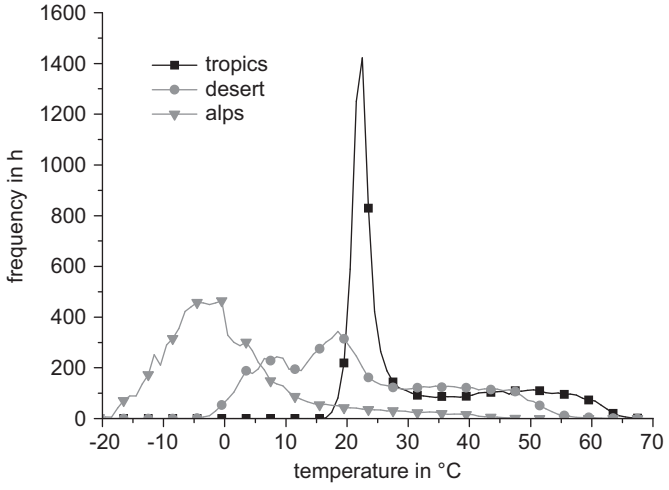

Fig. 2. Frequency distributions of the average temperatures of all measured modules at the different test sites for one year.

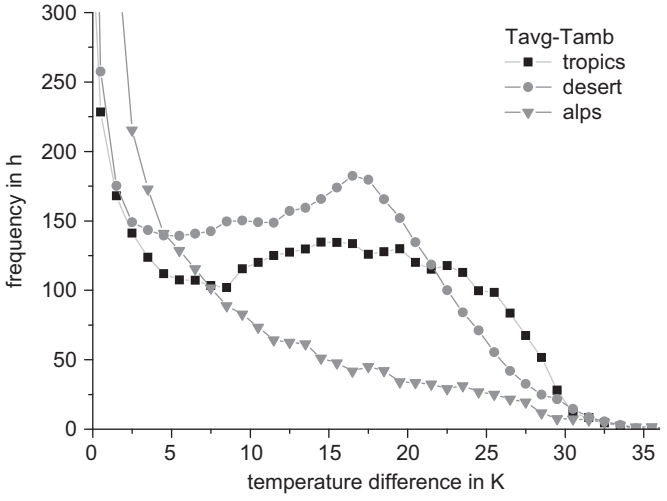

Fig. 3. Frequency distributions of the difference between the average module temperatures and the ambient temperatures at the different test sites for one year.

Another model was derived from the energy balance for a solar thermal collector by David Faiman [5]

$$T_{mod} = T_{amb} + \frac{G}{U_0 + U_1 v} \quad (2)$$

T_{mod} is the module temperature, T_{amb} the ambient temperature, G the global irradiation in the plane of incidence, v the wind speed, U_0 [W/°C m^2] is a coefficient describing the effect of the

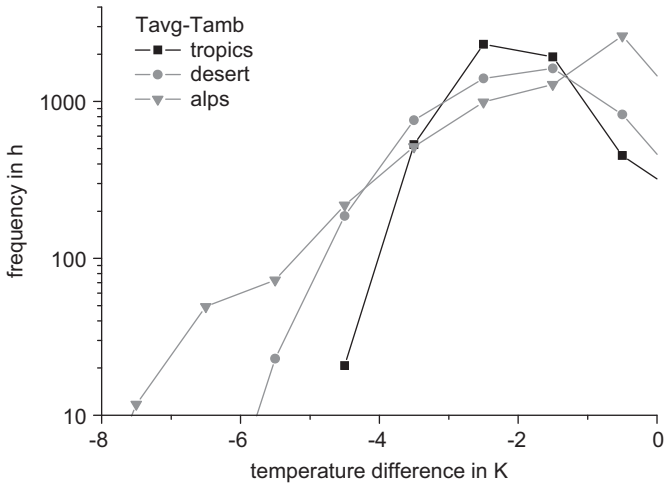

Fig. 4. Frequency distributions of the difference between the average module temperatures and the ambient temperatures at different test sites for one year, when the module temperature is lower than the ambient temperature.

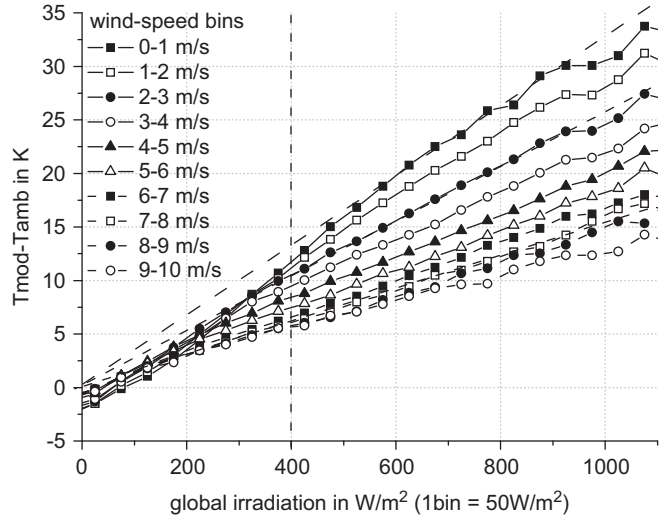

Fig. 5. Difference between the average module temperatures and the ambient temperatures at the desert test site in the Negev as a function of the global irradiation in the plane of the array for different wind speed bins for one year. Several dashed straight lines starting at the origin are drawn as guidance for the eye.

radiation on the module temperature, while U_1 describes the cooling by the wind and has the dimension Ws/°C m^3.

Both models neglect the influence of the infrared irradiation exchange with the cold sky and the natural convection (buoyancy), which is noticeable at low wind-speed and low irradiation (see Fig. 5). We neglect the back-insulation by roof-mounting and BIPV, which results in higher module-temperatures as well and refer to literature [4], [6], and [7].

5. Modeling of crystalline silicon module temperatures

The results for the evaluation of the model-parameters for the seven different c-Si modules after two years of monitoring in the Negev-desert and a half year in the alpine site are listed in Table 1. The difference of the coefficients for the different module types evaluated from two years data in the desert is not large for both models. This difference is smaller in King's model (about 1% for the irradiation influence and about 5% for the wind impact). The Faiman model seems to be more sensitive to climate and module type. This holds true for the wind impact in the Alps, which results in variations between the module type of about 5% for the irradiation influence, and up to 16% for the wind impact. The potential failures for low wind speed can be seen in the wind dependent evaluation of the model-parameters shown in Fig. 6. The irradiation influence is more pronounced for low wind velocities while the U_1 is clearly smaller than the average.

Table 1
Coefficients for the two module-temperature models using 2 full years' data in the Negev and a half-year in the Alps.

Sun Module #	King Negev 1st year	a [–] Negev 2nd year	Alps	Faiman Negev 1st year	U_0 [W/Km^2] Negev 2nd year	Alps
1	3.41	3.42	3.53	29.48	28.01	29.72
2	3.37	3.34	3.67	27.25	26.57	31.95
3	3.40	3.41	3.54	28.03	27.52	27.02
4	3.38	3.41	3.65	28.03	27.87	30.91
5	3.37	3.37	3.56	26.13	26.59	27.03
6	3.31	3.31	3.33	23.68	24.47	22.38
7	3.35	3.38	3.54	25.86	27.01	27.27
Average	3.37	3.38	3.55	26.92	26.86	28.04
Std deviation	0.03	0.04	0.11	1.89	1.20	3.19
Std dev %	1.02	1.19	3.15	7.01	4.48	11.38

Wind Module #	King Negev 1st year	b [s/m] Negev 2nd year	Alps	Faiman Negev 1st year	U_1 [Ws/Km^3] Negev 2nd year	Alps
1	0.14	0.14	0.11	6.50	7.28	5.95
2	0.12	0.12	0.10	5.72	5.03	6.78
3	0.14	0.14	0.14	6.73	6.69	9.21
4	0.13	0.13	0.13	6.14	6.24	8.93
5	0.13	0.13	0.14	6.13	5.75	8.89
6	0.14	0.13	0.14	6.34	5.95	6.92
7	0.12	0.12	0.12	6.12	5.83	7.73
Average	0.13	0.13	0.12	6.24	6.11	7.77
Std. deviation	0.01	0.01	0.02	0.32	0.72	1.27
Std. dev. %	4.15	6.68	13.17	5.19	11.81	16.34

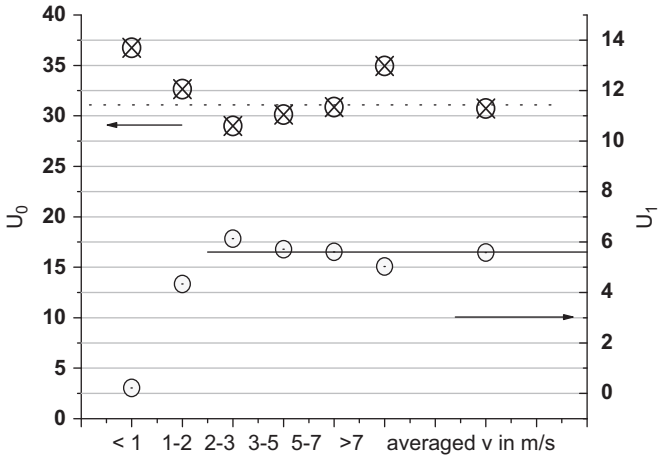

Fig. 6. The parameters for the Faiman model evaluated for the average of the seven measured module temperatures and different wind speed ranges (see Fig. 5) for one year in the Negev. The horizontal lines show the averages for wind speed values above 2 m/s.

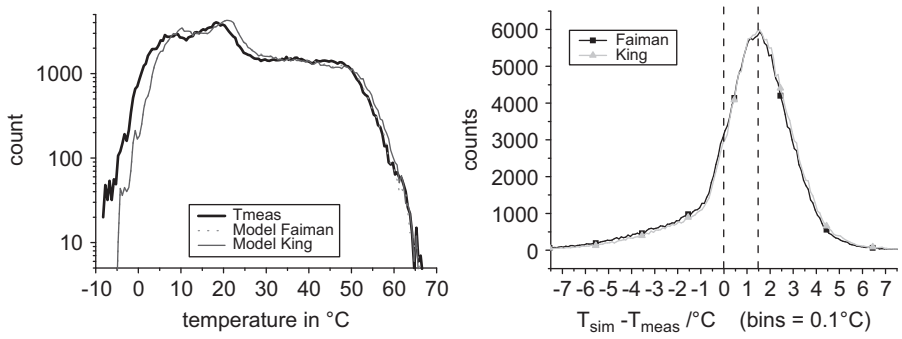

Fig. 7. Histogram of the predicted and measured module temperatures and of the difference between module temperature and the ambient temperature at the test site in the Negev for both considered models (unfiltered data).

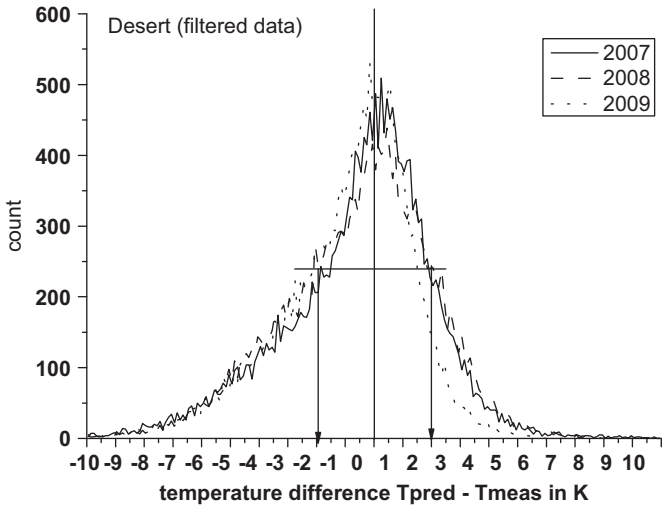

Fig. 8. Histogram of the difference between the predicted (Faiman model) and the measured module temperatures for the filtered data set (only for $G > 400$ W/m^2, low thermal inertia) at the test site in the Negev for 3 consecutive years.

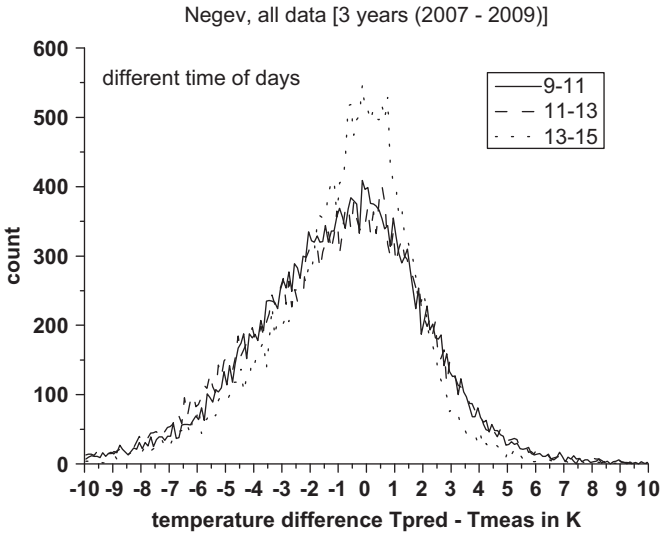

Fig. 9. Histogram of the difference between the predicted (Faiman model) and the measured module temperatures for the filtered data set (only for $G > 400$ W/m^2, low thermal inertia) at the test site in the Negev during morning, noon and afternoon integrated for 3 consecutive years.

The prediction of the module temperature works very well in both cases and shows the expected deviation at low values due to the neglected irradiation cooling, which results in a general shift of the predicted module temperature by 1.5 K (see Fig. 7). In order to avoid errors caused by the modules' thermal mass, the monitored data were partly filtered for the evaluation of the correlation between module temperature and climatic conditions. In this case, all data taken during the following conditions, as the standard for evaluation of the NOCT requires, were rejected:

- Irradiance value below 400 W/m^2.
- Data in a 10-min interval after the irradiance varied by more than 10% from the maximum value to the minimum value recorded during that 10-min period.
- Data in a 10-min interval after a change in wind speed of more than +200% and −50%.

In this case, the distribution of the difference between predicted and measured module temperature with a FWHM of about 4 K around zero was achieved, which does not change very much from year to year (Fig. 8) and even not between morning and afternoon (Fig. 9). We could only recognize less scattering during noon.

Fig. 10 shows the scattering of all the data and data that has only/just been filtered from one year including the effects of thermal inertia, IR radiation losses, and rapidly changing irradiation. Maximum variations are +/−10 °C at 40 °C measured module temperature. The over-estimation of the temperatures at low irradiation levels or during night time (low temperature range) can be recognized easily.

6. Modeling of thin-film modules

One year temperature histograms from Cadarache (France) are shown in Fig. 9. The maximum temperatures differed up to 10 K depending on the thin-film module type. The lowest temperatures were found for the crystalline Silicon module (serving as reference) and the two amorphous Silicon modules based on flexible substrates.

The coefficients for the Faiman model are listed in Table 2. CIS and CdTe show the biggest effect of the solar irradiation. The flexible a-Si modules have the highest wind impact coefficients.

The Faiman model parameters from Table 2 were evaluated from the Cadarache data and used for the prediction of the module temperatures in Cadarache and Freiburg for validation of the model by comparison with the measured temperatures.

The application of the model for a fictive exposure in the Negev yields the temperature histograms in Fig. 12. The spread in maximum temperatures looks similar to that in Fig. 11, but the flexible a-Si modules show lower maximum temperatures because of the higher wind velocities in the desert. Such histograms are especially useful for

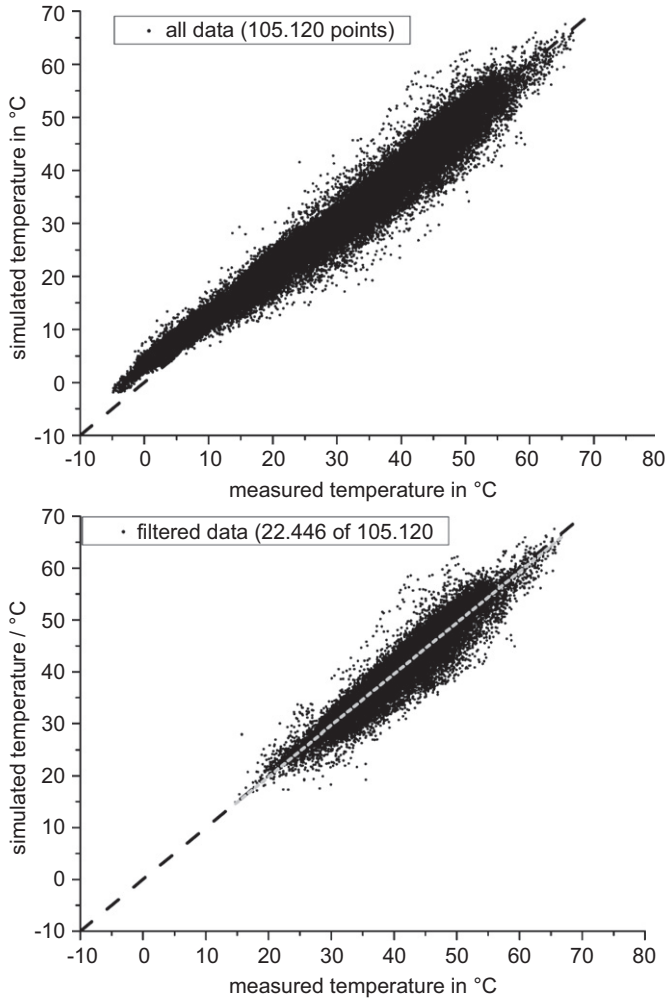

Fig. 10. The predicted versus the measured module temperatures for one year. All measured data are displayed in the top diagram. The data in the bottom diagram are the ones remaining after filtering according to the conditions of IEC61215 10.5, as described in the text. The dashed line represents the ideal straight line with slope 1.

Table 2
Faiman coefficients for the different thin-film module types.

	U_0	U_1
a-Si 1	25.73	10.67
a-Si 2	25.26	4.27
a-Si 3	26.16	4.25
a-Si 4	25.79	5.78
CIS 1	23.09	3.11
CIS 2	22.19	4.09
CdTe	23.37	5.44
c-Si-reference	30.02	6.28

the evaluation of the stresses on the modules for the design of accelerated durability tests.

7. Modeling by principal component analysis

The principal component analysis can be used for the identification of main influence factors. We used the software package "Unscrambler" [8] for analysis of the monitored climatic data.

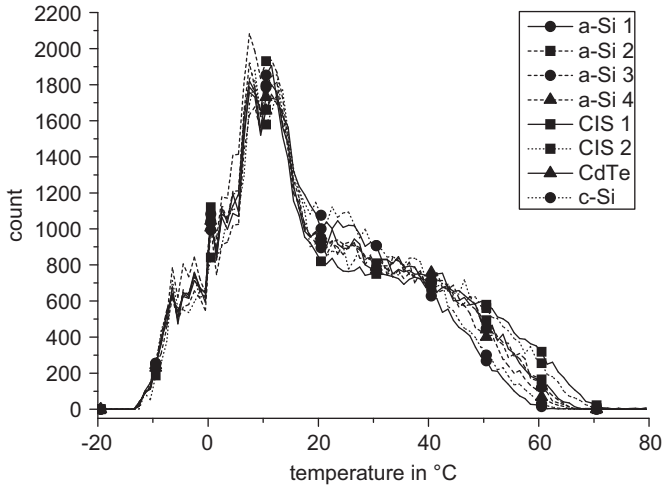

Fig. 11. Histogram of eight measured module temperatures for one year exposure in Cadarache (France).

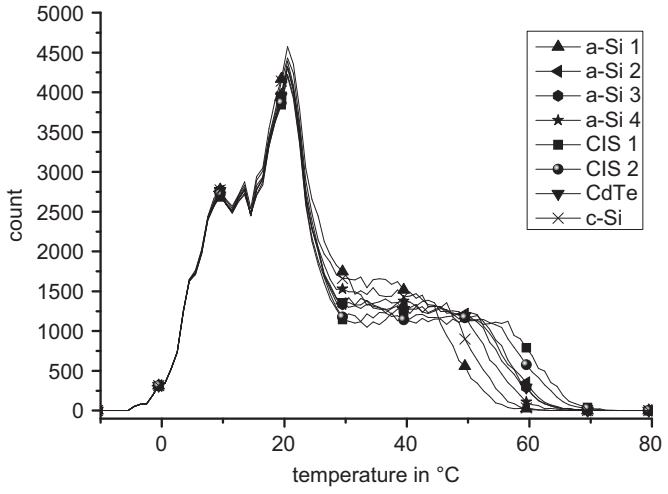

Fig. 12. Histogram of the predicted module temperatures for seven thin-film modules and one c-Si reference for one year in the Negev (Israel).

A typical result is shown in Fig. 13, which is a graphical display of the variables in four quadrants. The variables grouped at the right end of the PC1-axis show a high positive correlation: the module temperature, the ambient temperature, the irradiation. The wind direction seems to be positively correlated as well – which is an effect of the local conditions – while the wind-speed and the air-mass (as measure for the angle of incidence of the solar radiation) are clearly anti-correlated. The factors for the independent variables derived from the PCR can be used for modeling the dependent variable as a function of the independent variables. The results of the predicted versus measured module temperatures for a period of two weeks are presented in Fig. 14. Data was acquired on the accredited test site for NOCT-measurements at the Testlab PV-Modules of Fraunhofer-ISE in Freiburg. The correlation is as good as for the analytical models in the previous chapters and even no systematic deviations for low irradiance and high irradiance can be found.

8. Modeling of NOCT

The so-called Nominal Operating Cell Temperature (NOCT), which is defined by IEC standards [2] in point 10.5, should

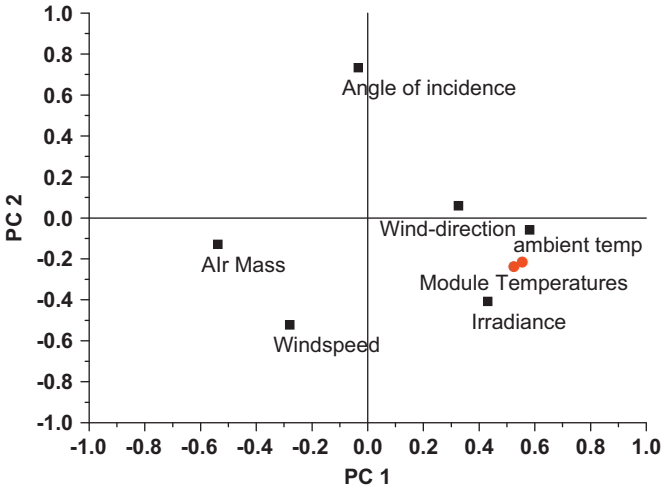

Fig. 13. Results of a principal component analysis with the module temperature as dependent variable from 2009/03/28 to 2009/04/14 NOCT-measurement.

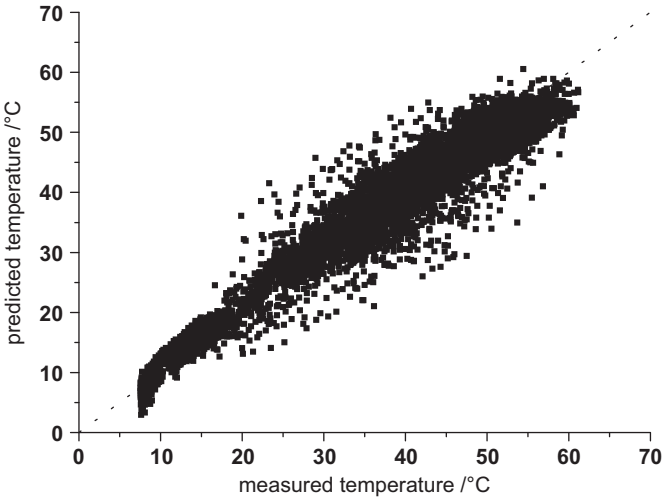

Fig. 14. Predicted versus measured module-temperature for the time-period from 2009/03/28 to 2009/04/14. The dashed line represents the ideal straight line with slope 1.

characterize the temperature dependence of the module and should allow the estimation of the performance and the energy yield of modules over time. These conditions are not really abundant in reality.

We used the module temperatures, which were measured at the back-sheet of 7 c-Si modules, which were kept near the maximum power point by means of resistive loads and which had been monitored during 25 months in the Negev desert, and filtered the data according to this standard. The result has 53 valid values out of a data pool of 219168 sets as shown in Fig. 15. The scattering of the values is considerable. The average temperature value was 43.7 °C, while the most probable temperature was 45.5 °C (note that the modules were exposed at maximum power). This value, which we now call Realistic Operational Module Temperature (ROMT) for better distinction from the Nominal Operational Cell Temperature (NOCT), could be evaluated from the model (Eq. (2)), too

$$ROMT = 20\ ^{\circ}\mathrm{C} + 800\ W/m^2/(U_0 + U_1^* 1\ m/s) \quad (3)$$

The results of ROMT, calculated according to the Faiman model (Eq. (3)), which can be seen in Table 3, are in very good agreement

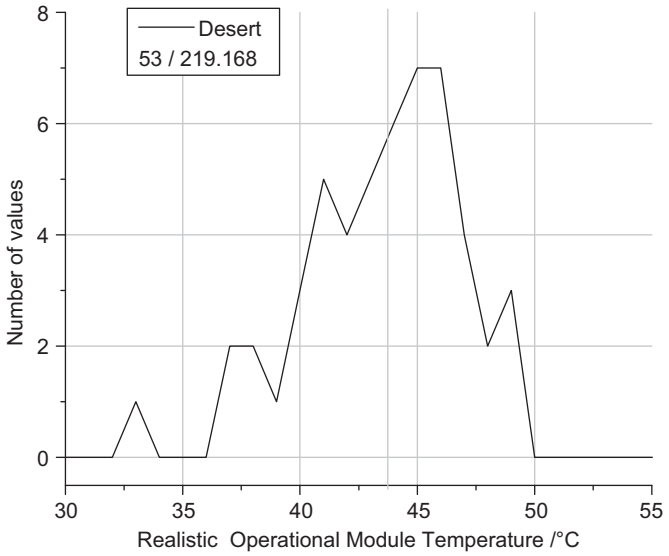

Fig. 15. Histogram of the average ROMT values (in 1 K bins) evaluated from 25 months monitoring of the c-Si modules exposed with a resistive load in the Negev (Israel). The average is 43.7 °C.

Table 3
ROMT values of c-Si modules evaluated from the Faiman model from 1 month or 1 year monitoring.

	U_0	U_1	period	ROMT/°C
Desert	28.7	5.89	1year	43.12
(Negev)	29.3	5.66	1month	42.88
Mountain	27.6	6.08	1year	43.75
(Alpes)	22.2	5.96	1month	48.41

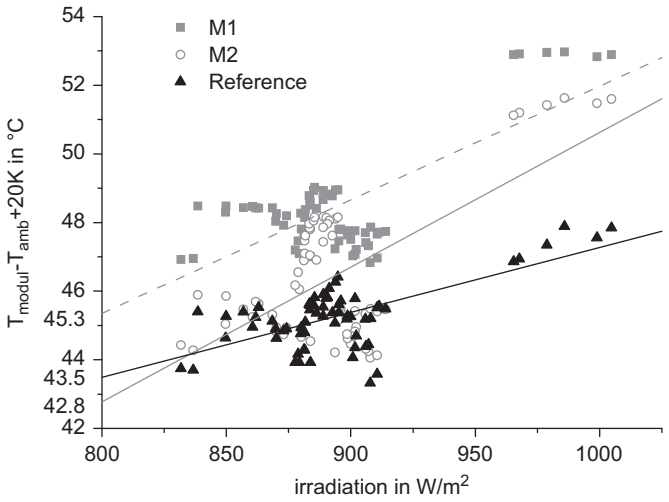

Fig. 16. Evaluation of the NOCT of three modules exposed with open circuit evaluated from NOCT testing. The data points in the figure are valid values according to IEC61215 (above 800 W/m^2 irradiation). The resulting NOCT values are 45.3 °C for M1, 42.8 °C for M2 and 43.5 °C for the reference module are determined by using a regression analysis (see straight lines) and interpolation to 800 W/m^2.

with the monitored data used for Fig. 15, even after only one month monitoring in the desert. The colder mountain climate might require longer measurement periods for obtaining comparable results.

The modules should be exposed with open circuit for the determination of the NOCT according to the present IEC standards, which leads to a higher cell-temperature, because the electrical power is not extracted but is converted into heat. The ambient temperature should be 20 °C+/−15 K and the wind impact should be negligible (v=1+/−0.75 m/s). The results for the investigation of the wind impact shown in Figs. 5 and 6 do not recommend focusing on these situations, because the effect of module cooling by radiation and natural convection is most pronounced but not taken into account directly. Furthermore the wind direction is restricted. We refer to the standards [2] for the other border conditions and the evaluation and correction procedures. It is not easy to collect sufficient data under bad weather conditions (high wind and low sun) as happens in the central European fall and winter seasons. Fig. 16 shows an example for the analysis of 3 modules from May 2009. All valid temperature values at irradiance values above 800 W/m^2, which had passed the filtering described above, are displayed in order to demonstrate the scattering of the data up to +/−2 K for the temperature or +/−50 W/m^2 for the irradiation. A linear regression analysis for all valid data between 400 and 1000 W/m^2 must be performed (see straight lines in Fig. 16) in order to interpolate the value at 800 W/m^2 irradiation.

Modeling the NOCT by means of principle component regression (PCR) is possible by using the weighting factors evaluated and shown in Fig. 13 for the climate parameters defined in the IEC standards: ambient temperature, irradiance and wind-speed and wind direction, but without filtering for special climatic conditions. Using this procedure for the prediction of the module NOCT with the data displayed in Fig. 16 gives values for the NOCT of 45.7 °C (module 1) and 43.6 °C (module 2), while the values obtained by the IEC-standard procedure were 45.3 and 42.8 °C, respectively. This small deviation suggests the further investigation of the application of such mathematical tools like the principle component regression.

9. Proposal for the evaluation of the NOCT

The normal working conditions for PV-modules are operations at the maximum power point. We propose to avoid the characterization at open circuit conditions. The operating cell temperature would be lower than determined according to IEC61215 or 61 646 because of the extraction of the electrical power. A higher electrical efficiency would result in a lower module and cell temperature. The temperature measurements might need to be performed at the back-side of some different cells in order to detect and avoid hot-spot effects.

We could imagine that the ROMT could be evaluated during the outdoor exposure test at the maximum power point conditions for 60 kWh/m^2 solar irradiation, as it is required by IEC61215 clause 10.8. Fig. 16 shows the results for the evaluation of the NOCT for the Fraunhofer ISE reference NOCT module (crystalline silicon cells) during outdoor exposure according to the NOCT standard (open circuit) during one year, but using only data at irradiance values above 400 W/m^2; no data in a 10-min interval after the irradiance varied by more than 10% from the maximum value to the minimum value recorded during that 10-min period and no data in a 10-min interval after a change in wind speed of more than +200% and −50%.

The data were compiled until the dose of incident solar energy reached 60 kWh/m^2 and then used for modeling the module temperature according to Eq. (2) and evaluation of a NOCT according to Eq. 3. The differences between both methods are much smaller than the errors discussed in Fig. 16, in spite of the remarkable seasonal variation of the model parameters U_0 and U_1, showing the increased impact of the irradiation on the module temperature during winter and at higher wind speeds. Suitable NOCT values could be evaluated even during winter time, while no results could be achieved in the traditional way (Fig. 17).

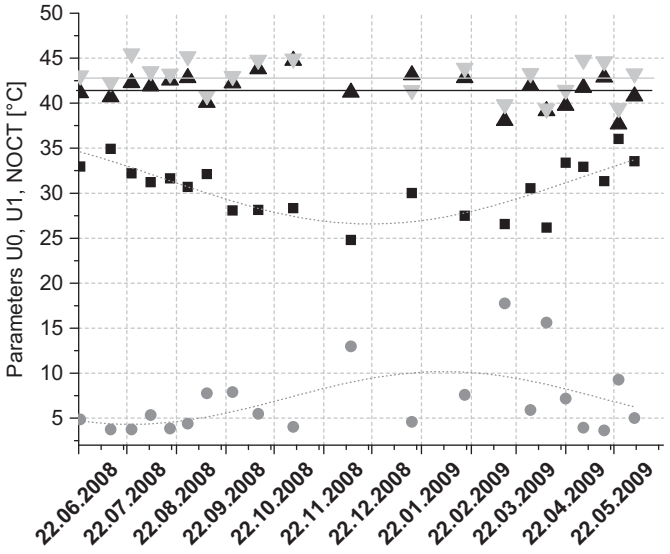

Fig. 17. Evaluation of the exposed reference module's NOCT in bins of 60 kW/m^2 irradiation according to the standard IEC61215 (gray triangles) and from module temperature modeling (Black triangles) according to eq. (2) with data from the same period. The parameter U_0 is shown in black squares and the U_1 in gray circles. Yearly average values: U_0=30.6, U_1=6.9, NOCT (modeled) 41.5 °C, NOCT (traditional) 42.8 °C (indicated as straight lines in the diagram).

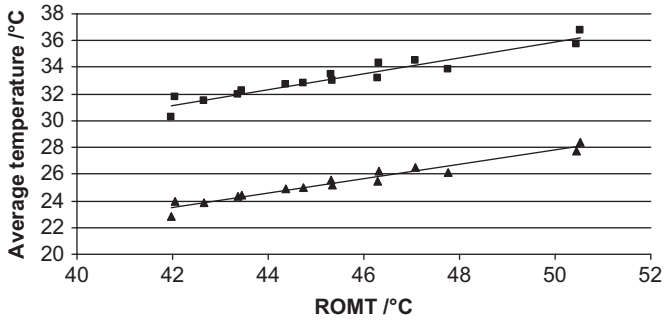

Fig. 18. Calculated yearly average temperature for the modules listed in Table 5 for the locations Boulder, USA (triangles) and Desert Rock, USA (squares) as a function of the modeled ROMT-value. The straight lines are linear regression fits.

Table 4
Modeled ROMT for thin-film modules (at mpp).

	U_0	U_1	ROMT
a-Si 1	25.73	10.67	41.98
a-Si 2	25.26	4.27	47.09
a-Si 3	26.16	4.25	46.31
a-Si 4	25.79	5.78	45.34
CIS 1	23.09	3.11	50.53
CIS 2	22.19	4.09	50.44
CdTe	23.37	5.44	47.77
c-Si	30.02	6.28	42.04

The calculation of the ROMT of thin-film modules (exposed at mpp) using the model discussed in the previous chapter yielded the ROMT values shown in Table 4. The model can be used for simulation and prediction of the module temperature and the energy yield at locations with known time series of the climatic data, ambient temperature, solar irradiation and wind-speed. Examples can be found in Table 5. We calculated yearly average temperatures for different module types at different locations for which time series of

Table 5
Simulated average module-temperatures for one year at different locations (Cadarache: 30.07.2007–17.06.2007, Köln, Negev, Serpong, Zugspitze: 01.06.2007–31.05.2008, 2007 for the other locations).

Parameter U_0				28.01	26.57	27.52	27.87	26.59	24.47	27.01	25.73	25.26	26.16	25.79	23.09	23.19	23.37	**30.02**
Parameter U_1				7.28	5.03	6.69	6.24	5.75	5.95	5.83	10.67	4.27	4.25	5.78	3.11	4.09	5.44	**6.28**
				42.67	45.32	43.38	43.45	44.47	46.30	44.36	41.98	47.09	46.31	45.34	50.53	50.44	47.77	**42.04**
	Yearly average ambience			**Yearly average module temperature in °C**														
Location	***G* in W/m²**	***Tamb* in °C**	***v* in m/s**															
Bondville (USA)	168.75	11.90	.91	22.62	24.1	22.97	23.15	23.63	23.85	23.51	21.59	24.94	24.77	23.74	26.69	25.83	24.4	**22.84**
Boulder (USA)	189.28	11.89	3.42	23.89	25.52	24.29	24.46	25.04	25.45	24.89	22.87	26.48	26.22	25.22	28.42	27.72	26.13	**23.99**
Cadarache (France)	237.06	10.79	1.63	27.9	28.48	29.69	28.35	29.22	29.92	29.02	27.07	30.82	30.43	29.5	33.05	32.55	30.77	**27.79**
Desert Rock (USA)	236.26	18.98	4.11	31.54	33.44	31.98	32.22	32.84	33.16	32.69	30.24	34.54	34.31	32.99	36.81	35.74	33.88	**31.79**
Fort Peck (USA)	159.46	6.77	4.48	18.32	19.71	18.64	18.82	19.26	19.47	19.15	17.36	20.5	20.34	19.36	22.14	21.33	19.98	**18.53**
Goodwin Creek (USA)	180.21	16.63	2.02	29.59	31.23	29.99	30.15	30.5	31.21	30.6	28.59	32.2	31.92	30.95	34.14	33.5	31.9	**29.66**
Koln (Germany)	130.16	12.15	1.64	24.19	25.43	24.51	24.6	25.11	25.6	24.97	23.58	26.21	25.93	25.31	27.73	27.42	26.19	**24.11**
Negev (Israel)	269.91	18.07	3.02	34.03	36.3	34.58	34.83	35.62	36.14	35.42	32.54	37.62	37.28	35.85	40.29	39.27	37.06	**34.22**
Penn State (USA)	151.38	9.37	3.23	20.69	22.14	21.04	21.2	21.7	22.03	21.58	19.75	22.99	22.78	21.85	24.73	24.03	22.61	**20.82**
Serpong (Indonesia)	188.94	26.88	1.00	42.87	44.35	43.27	43.31	44.03	44.9	43.82	42.48	45.35	44.91	44.37	47.28	47.23	45.73	**42.51**
Sioux Falls (USA)	165.03	8.20	4.42	18.55	20.00	18.89	19.08	19.54	19.74	19.43	17.52	20.83	20.66	19.64	22.53	21.67	20.27	**18.79**
Zugspitze (Germany)	128.33	−0.67	2.70	14.08	15.61	14.47	14.59	15.19	15.72	15.03	13.27	16.54	16.24	15.41	18.4	17.91	16.41	**14.06**

the climatic data were available by using the Faiman model and the module-type specific parameters U_0 and U_1. These average temperatures seem to be proportional to the ROMT values simulated by equation (3) as shown in Fig. 18. In this way a first impression of the thermal stress and the expected electrical energy can be obtained, but a transient comprehensive simulation of the energy yield is still needed. The modeled module temperatures can be used for this purpose.

10. Conclusions

A statistical model based on principal component analysis and a simple analytical model for the evaluation of the temperature of PV-modules from climatic data (ambient temperature, global solar irradiation in the plane of array and wind speed) was investigated. The parameters which describe the effects of the solar irradiation and the wind speed for different cell technology and module design must be evaluated from monitored outdoor exposure data. One month monitoring of 5 min averages seem to be sufficient at favorable climatic conditions. The impact of radiation cooling and natural convection can be neglected for wind speeds above 2 m/s. The main effect of radiation cooling can be found during night time which is not relevant for the solar energy gain. The effect of wind gusts and fast temperature changes has to be excluded.

The models are useful for the simulation of the transient temperature loads on modules at locations and periods for which the needed weather data are available. These simulation data can be used for estimation of the energy gain of different module types or for estimation of the thermal stress on the materials. Further work is necessary to take into account the effect of building integration on the module temperatures.

A simpler way to determine the Nominal Operating Cell Temperature (NOCT) simultaneously during the IEC outdoor exposure testing (60 kWh/m^2) can be proposed.

Acknowledgements

The work was partly funded by the German Federal Ministry for the Environment, Nature Conservation and Nuclear Safety (BMU FKz 0329978), the European Commission (Project PERFORMANCE) and sponsored by the industrial partners Scheuten Solar, Schott Solar, Solarfabrik, Solarwatt, Solar World and Solon.

The authors are grateful to Sarah Kurtz, Antoine Guerin de Montgareuil and John Wohlgemuth for stimulating discussions and wish to thank Antoine Guerin de Montgareuil, David Faiman and Werner Herrmann for providing outdoor measurement data.

References

[1] M. Koehl, M. Heck, D. Philipp, K.-A. Weiss, C. Ferrara, W. Herrmann, Indoor and outdoor weathering of PV-modules, in: Proceedings of the SPIE Conference 7048, San Diego, 2008.
[2] IEC 61215 ed. 2 (Crystalline Silicon Thin-Film Terrestrial Photovoltaic (PV) Modules—Design Qualification and Type Approval) and IEC 61646 ed. 2 (Thin-Film Terrestrial Photovoltaic (PV) Modules—Design Qualification and Type Approval).
[3] E. Skoplaki, J.A. Palyvos, Operating temperature of photovoltaic modules: a survey of pertinent correlations, Renew. Energy 34 (2009) 23–29.
[4] D.L. King, W.E. Boyson, J.A. Kratochvil, Photovoltaic Array Performance Model, Sandia National Laboratories, 2004 SAND2004-3535.
[5] D. Faiman, Assessing the outdoor operating temperature of photovoltaic modules, Prog. Photovolt.: Res. Appl. 16 (2008) 307–315.
[6] S. Kurtz et. al., Evaluation of high-temperature exposure of photovoltaic modules, Prog. Photovolt.: Res. Appl., accepted for publication.
[7] J. Oh, G. TamizhMani, Ernie Palomino, Temperatures of Building Applied Photovoltaic (BAPV) Modules: Air Gap Effects, in: Proceedings of the SPIE Conference 7773, San Diego, 2010.
[8] The Unscrambler: 〈http://www.camo.com/rt/Products/Unscrambler/unscrambler.html〉.